AD-A066 485   AEROSPACE CORP EL SEGUNDO CALIF AEROPHYSICS LAB   F/G 17/8
                   FIGURES OF MERIT TO CHARACTERIZE INTEGRATING IMAGE SENSORS.(U)
                   JAN 79 E F CROSS, G I SEGAL   F04701-78-C-0079
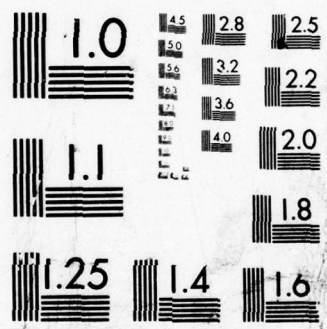UNCLASSIFIED   TR-0079(4940-01)-1   SAMSO-TR-79-17   NL

| OF |
AD
AD66485

END
DATE
FILMED
5--79
DDC

MICROCOPY RESOLUTION TEST CHART

NATIONAL BUREAU OF STANDARDS-1963-A

(12) **LEVEL** II

Figures of Merit to Characterize Integrating Image Sensors

E. F. CROSS
Aerophysics Laboratory
and
G. I. SEGAL
Space Sciences Laboratory
Laboratory Operations
The Aerospace Corporation
El Segundo, Calif. 90245

15 January 1979

Interim Report
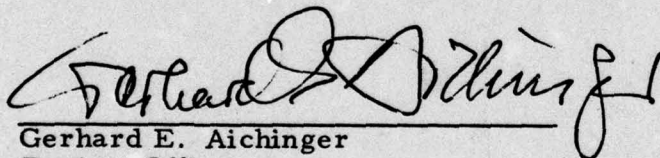
D D C
RECEIVED
MAR 28 1979
B

Prepared for

SPACE AND MISSILE SYSTEMS ORGANIZATION
AIR FORCE SYSTEMS COMMAND
Los Angeles Air Force Station
P.O. Box 92960, Worldway Postal Center
Los Angeles, Calif. 90009

79 03 23 061

Gerhard E. Aichinger
Project Officer

FOR THE COMMANDER

Frank J. Bane, Chief
Contracts Management Office

REPORT DOCUMENTATION PAGE		READ INSTRUCTIONS BEFORE COMPLETING FORM
1. REPORT NUMBER SAMSO-TR-79-17	2. GOVT ACCESSION NO.	3. RECIPIENT'S CATALOG NUMBER
4. TITLE *(and Subtitle)* FIGURES OF MERIT TO CHARACTERIZE INTEGRATING IMAGE SENSORS .		5. TYPE OF REPORT & PERIOD COVERED Interim rept.
		6. PERFORMING ORG. REPORT NUMBER TR-0079(4940-01)-1
7. AUTHOR(s) Edward F. Cross and Gary I. Segal		8. CONTRACT OR GRANT NUMBER(s) F04701-78-C-0079
9. PERFORMING ORGANIZATION NAME AND ADDRESS The Aerospace Corporation El Segundo, Calif. 90245		10. PROGRAM ELEMENT, PROJECT, TASK AREA & WORK UNIT NUMBERS
11. CONTROLLING OFFICE NAME AND ADDRESS Space and Missile Systems Organization Air Force Systems Command Los Angeles, Calif. 90009		12. REPORT DATE 15 January 1979
		13. NUMBER OF PAGES 22
14. MONITORING AGENCY NAME & ADDRESS*(if different from Controlling Office)* 25p.		15. SECURITY CLASS. *(of this report)* Unclassified
		15a. DECLASSIFICATION/DOWNGRADING SCHEDULE

16. DISTRIBUTION STATEMENT *(of this Report)*

Approved for public release; distribution unlimited

17. DISTRIBUTION STATEMENT *(of the abstract entered in Block 20, if different from Report)*

DDC
RECEIVED
MAR 28 1979
B

18. SUPPLEMENTARY NOTES

19. KEY WORDS *(Continue on reverse side if necessary and identify by block number)*

Camera-Tube Performance   Vidicon Standards
Image Sensors
Image Standards
Imagery Figures of Merit
Television Performance Standards

20. ABSTRACT *(Continue on reverse side if necessary and identify by block number)*

Criteria and laboratory techniques used to measure the performance of integrating image sensors are described. The integrating image sensor has a sensing layer that continually monitors the field of view and an electronic mechanism that sequentially reads out the integrated signal on an elemental basis. Test procedures are given for determining transfer characteristics, spatial response, spectral response, response uniformity, and image retention of these integrating image sensors.

DD FORM 1473
(FACSIMILE)

79 03 23 061
409 367

CONTENTS

FIGURES

I. INTRODUCTION

The increased use of television systems to obtain radiometric, spatial, and gradient data has necessitated the formulation of figures of merit that define image-sensor performance. Criteria and laboratory techniques used to measure the operational parameters for integrating image sensors are described. An integrating image sensor has a sensing layer that continually monitors the field of view and an electronic mechanism that sequentially reads out the integrated signal on an elemental basis. This characterization of the sensor is applicable for nearly all vidicon camera tubes and most staring arrays regardless of their spectral response characteristics. Much of the terminology and measurement techniques described in this paper was taken from the performance criteria formulated by the IRIS Specialty Sub-group on Infrared Camera Tube Standards.[1,2]

---

[1] Proc. IRIS, Vol. 8, pp. 51-59. 1963.
[2] Proc. IRIS, Vol. 10, pp. 49-55. 1966.

II. GENERAL APPROACH AND TERMINOLOGY

The integrating image sensor is a black box that produces output signals corresponding to the scene at the optical image plane. Figures of merit derived for each image sensor are independent of such associated equipment as optics and video electronics. Windows of any separate Dewar assembly used to cool the image sensor are included with the optics unless the Dewar is an integral part of the image-sensor construction.

Operating voltages and currents that control image quality must be held constant during all the tests. It may be desirable to obtain measurements at more than one set of operating conditions because selected image-sensor characteristics can be optimized at the expense of others. These measurements are important in describing trade-off options for the comparative evaluation of various types of image sensors.

The terms sensing layer or retina refer to the sensitive area of the image sensor. From sensing-layer voltage and current (V_{sl} and I_{sl}), measured with a dc voltmeter and dc nanoammeter, respectively, the operating point of the sensing layer is determined.

The input irradiance (H_i) is defined as the power density at the image plane and constitutes the total of the irradiance levels from the environment, background, and signal source with the image sensor removed. The signal irradiance (H_s) is that portion of H_i that originates from the signal source. Transmission efficiencies of any external filters necessary for device operation are not considered part of the image sensor. The signal irradiance (H_s) that reaches the sensing-layer window can be calculated from the following equation:

$$H_s = \frac{t_w t_f t_a t_n W_s}{4F^2(M + 1)^2 + 1}$$

-7-

where

t_o = transmission of system optics

t_f = transmission of external band-limiting filter

t_a = atmospheric transmission for optical path

t_n = transmission of any neutral density filter

F = f-number of the optical system

M = magnification of the optical system

W_s = radiant emittance in W/cm^2

With a standard blackbody source used as the calibration signal, the radiant emittance (W_s), as determined by the overall spectral bandpass of the image sensor, optics, and external spectral filters, is calculated from Planck's Law

$$W_s = 3.74 \times 10^{-12} \int_{\lambda_1}^{\lambda_2} \frac{1}{\lambda^5} \left(e^{1.438/\lambda T} - 1\right)^{-1} d\lambda$$

where

λ_2 = upper wavelength cutoff in centimeters

λ_1 = low wavelength cutoff in centimeters

T = blackbody source temperature in degrees Kelvin

All video signal measurements are obtained by monitoring the line video with a line-selector oscilloscope, as indicated by the video presentation in Fig. 1. Television monitors or equivalent video-display devices can be used to qualitatively adjust image-sensor performance but not to determine measurable parameters.

The relationship between the output video signal and input irradiance (H_i) is influenced by several factors. One of the most significant is the monitored $I_{s\ell}$ value. Figure 2 is an idealized pictorial representation of the line-selector oscilloscope waveforms for various conditions. Note that all
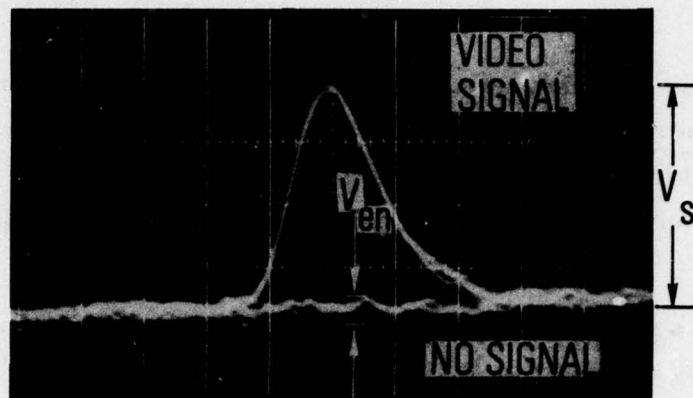
Fig. 1. Typical line-selector-oscilloscope
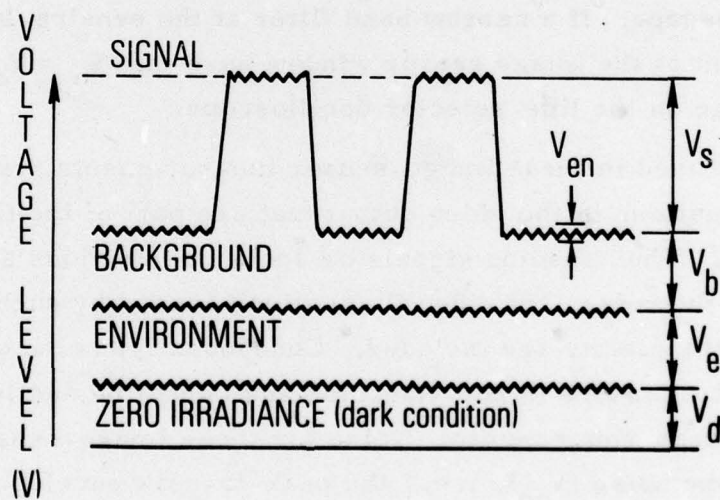presentation of video output

Fig. 2. Line-selector-oscilloscope video
presentation of irradiance levels

signal amplitudes are measured from the mean value of the high-frequency fluctuations, whereas output voltage levels on the ordinate are directly related to irradiance levels. The three typical video voltage outputs produced by dark, environmental, and multiple pattern plus background are evident in Fig. 2.

Under dark conditions the image-sensor window is covered by an opaque reflecting cap held at the sensing-layer temperature. The resultant voltage, monitored on the line-selector oscilloscope, is the dark voltage.

Under environment conditions the image-sensor window is covered by an opaque nonreflecting cap at the ambient temperature. In most cases this temperature is approximately 300 K. The voltage monitored on the line-selector oscilloscope is the environment voltage (V_e). For uncooled image sensors V_e is zero.

For the pattern-plus-background condition all opaque caps are removed, and the background and signal voltages (V_b and V_s) produced on the line-selector oscilloscope. If a narrow band filter at the sensing-layer temperature is placed in front of the image sensor window such that $V_b = V_e = O$, V_d is the no-signal voltage on the line-selector oscilloscope.

Noise, as used in these image-sensor measurements, is the random statistical fluctuations in the video output that are part of the fixed-pattern characteristics. Thus shading signals or spot imperfections are not considered part of the noise, but video fluctuations caused by such factors as sensing-layer granularity are included. Consequently, noise observed on the line-selector oscilloscope is non-Gaussian and cannot be easily expressed in terms of root-mean-square units. Noise for these image-sensor measurements is envelope noise (V_{en}), i.e., the peak-to-peak envelope of high-frequency voltage fluctuations viewed on the line-selector oscilloscope.

Five measurable parameters that can be used to describe the performance of the integrating image sensor are (1) transfer characteristics,

(2) spatial response, (3) spectral characteristics, (4) uniformity of response, and (5) image retention. Each one is discussed and techniques for reliably and accurately measuring these parameters are given.

III. TRANSFER CHARACTERISTICS

Transfer characteristics are used to describe the relationship between irradiance at the image plane and output signal of the image sensor. An image size is chosen that is significantly larger than the resolution element size of the image sensor. In general a suitable image size can be obtained in the laboratory with a standard blackbody source with an aperture 1.27 cm in diameter or greater. The temperature of the source is usually kept constant while neutral density filters of known transmissions are placed in front of the blackbody aperture. In this manner a wide range of V_s/V_{en}'s are readily produced without changing the blackbody temperature. The H_s can be calculated for each V_s/V_{en} value.

These measurements of transfer characteristics are presented as a log-log plot of H_s versus V_s/V_{en}. The linear slope of the resultant curve (γ) is given by the expression

$$\gamma = \frac{d \log V_s/V_{en}}{d \log H_s}$$

A typical transfer characteristic curve is shown in Fig. 3. The H_s that produces a V_s/V_{en} of 1 is defined as the noise equivalent irradiance (NEH). This derived quantity is a single value for specifying threshold detectivity for any given intergrating image sensor. The dynamic range (DR) is defined as the range over which γ is constant and is derived from the ratio of signal irradiance at sensing-layer saturation $[H_s(sat)]$ to NEH as given by the expression

$$DR = \frac{H_s(sat)}{NEH}$$

This derived quantity specifies the number of irradiance levels that a given intergrating image sensor can view simultaneously.
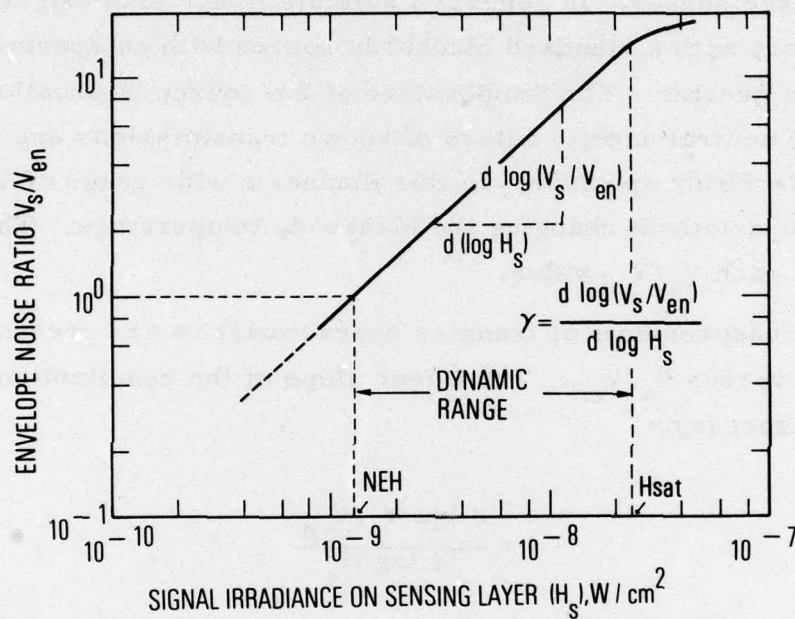
-13-

Fig. 3. Typical transfer characteristics curve

IV. SPATIAL RESPONSE

Spatial response characteristics are used to describe how image size and pattern at the sensing layer affect the output video signal. However, for the total range of integrating image sensors and various system resolution criteria, this image parameter cannot be specified by a single test. The three methods that have been formulated to accurately measure spatial response are integration element size, square-wave response, and separation of two subaperture spots. All three approaches have the advantage of requiring a minimum of special purpose equipment while providing reliable criteria for comparative evaluation of image sensor resolution.

Integration element size is the measure of image-sensor response to incident radiant power as image size is decreased to a point source and video output is held constant ($V_s/V_{en} = K$). For this measurement a mask with various circular apertures is placed in front of a blackbody source. First, the aperture size, focused at the image plane, is chosen to fill an area greater than the anticipated resolution element of the sensing layer. A blackbody temperature that produces a convenient V_s/V_{en} on a line-selector oscilloscope is selected. As aperture size is reduced, V_s/V_{en} remains constant until image dimensions approach the integration element size of the image sensor. From this point on, it is necessary to increase the W_s from the blackbody source to keep V_s/V_{en} constant as the apertures are made smaller.

Since the optical and blackbody parameters are known, image area (A_i and H_s) can be calculated. A log-log plot of $A_i H_s$ in watts as a function of A_i in square centimeters is shown in Fig. 4. If the linear slopes for both segments of the curve in this figure are extended until they intersect, the abscissa of this point is defined as the area of integration element size (A_e).

If A_i is larger than or equal to A_e, the image sensor is an irradiance detector, and the transfer characteristics are not influenced by image size.
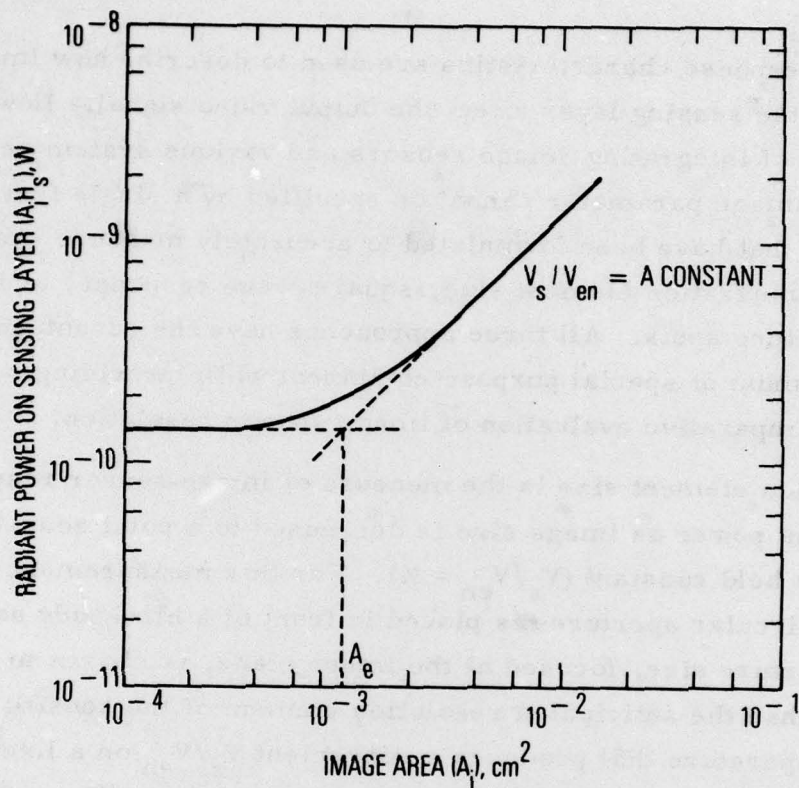
Fig. 4.   Typical integration element size curve

However, if A_i is smaller than A_e, the image sensor operates as a single-element detector, responsive to the radiant flux level (watts) with image size remaining constant. Then with the use of the product of A_e and NEH, the derived quantity of minimum detectable power per integration element (P_e^*) can be calculated. This parameter is also termed the minimum detectable watts per resolution element for an integrating image sensor.

The separation of two subaperture spots (significantly smaller in size than A_e) is a measure of the image-sensor video output modulation as the spacing between adjacent point images at the sensing layer is varied and V_s/V_{en} held constant. For this test masks with two circular apertures of equal size and variable spacings are placed in front of the blackbody source. Figure 5 is a photograph of the mask initially constructed to perform this measurement. This subaperture mask produces spot image pairs significantly smaller than A_e and that have center-line spacings from 0.813 to 0.216 cm. The signal irradiance is chosen to provide a convenient V_s/V_{en} on the line-selector oscilloscope. As shown in Fig. 6, the differential modulation voltage (V_m), corresponsing to the midpoint two subaperture images, is measured for each mask setting until peak and midpoint amplitudes are equal. The ratio of V_m to V_s is the modulation (M).

On the bases of known optical parameters and spot separation distances, the reciprocal of center-line distances between images ($1/d_s$) is calculated for each M. Figure 7 is a typical Cartesian coordinate plot of the variation of M in percentage as a function of $1/d_s$ in lines per millimeter.

The square-wave response is the measurement of output video modulation from the image sensor as spacings between bar pattern images at the sening layer are varied while H_s is held constant. In this test the total image pattern should fill at least 10% of the horizontal dimension of the sensing layer. A bar pattern mask similar to the one shown in Fig. 8 is maintained at or near ambient temperature, and then each bar pattern set is placed over
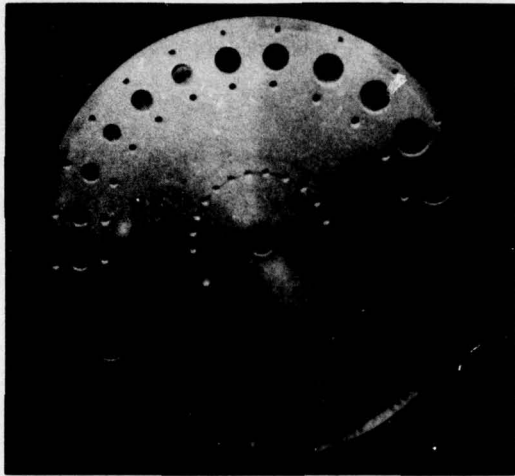
Fig. 5. Subaperture mask for
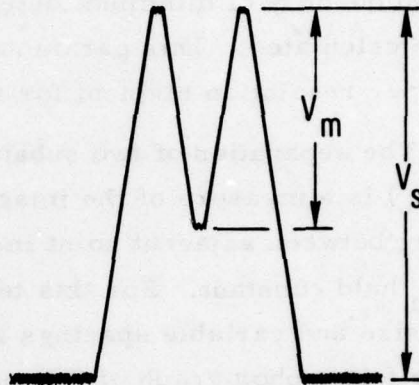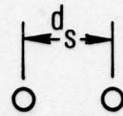measuring spot
separation

Fig. 6. Line-selector-oscilloscope
presentation of video from
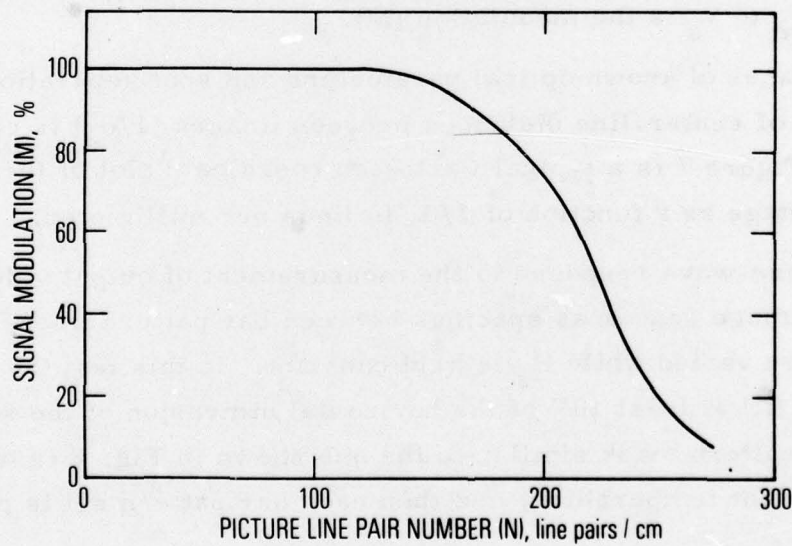subaperture spot images

Fig. 7. Typical curve for separation of two
subaperture spots

the blackbody source. These test stencils or plates should be of high emissivity and have at least three equally spaced vertical bar openings per set. As each imaged bar pattern is set in front of the blackbody source, the modulated V_s/V_{en} is measured on the line-selector-oscilloscope presentation (Fig. 9). With decreasing bar width, M decreases with reduced bar pattern width after remaining relatively constant for the initial large pattern widths.

The square-wave amplitude response is given as a plot of M expressed in percentage as a function line number per millimeter. The line number is the reciprocal of the width between pairs of imaged bars on the sensing layer (N). Figure 10 is a typical plot of square-wave response Cartesian coordinates, with M the ordinate and N the abscissa.
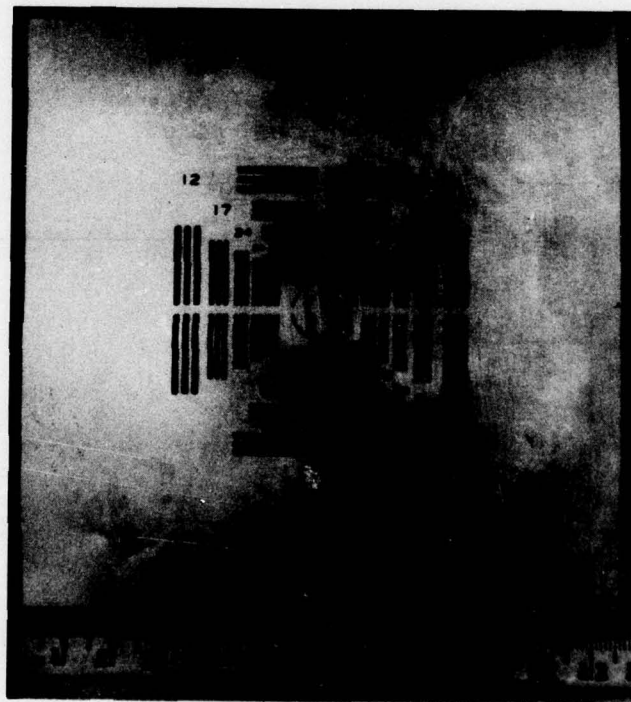
Fig. 8. Bar pattern mask for measuring
square-wave response

AT 100% MODULATION

$$V_m = V_s$$

AT 50% MODULATION

$$V_m$$

$$V_s$$
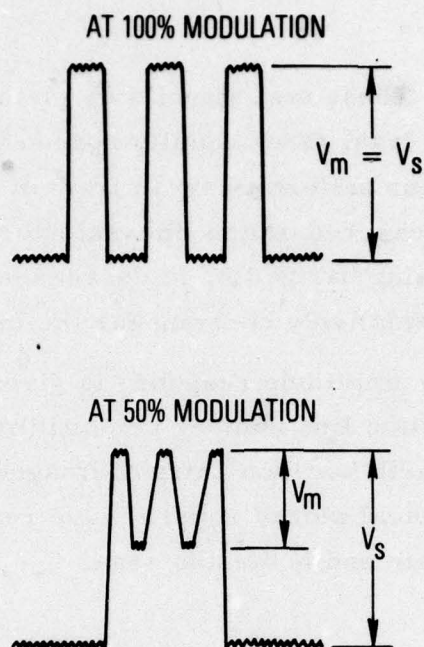
Fig. 9. Line-selector-oscilloscope
presentation of square-
wave response video

$$M = \frac{V_m}{V_s} \times 100$$

$$\frac{V_s}{V_{en}} = 6 \ (\text{constant})$$

MODULATION OF VIDEO SIGNAL (M), %

100

75

50

25

0

0   1   2   3   4

RECIPROCAL OF IMAGE SEPARATION DISTANCE (1 / d_s), lines/mm

Fig. 10. Typical square-wave response curve

V. SPECTRAL RESPONSE

Spectral response is the relationship between the spectral wavelength of signal irradiance and the output video signal. This measurement can be defined by the magnitude of H_s required to maintain the same V_s/V_{en} as the spectral wavelength of H_s is varied. A series of narrow band filters and a neutral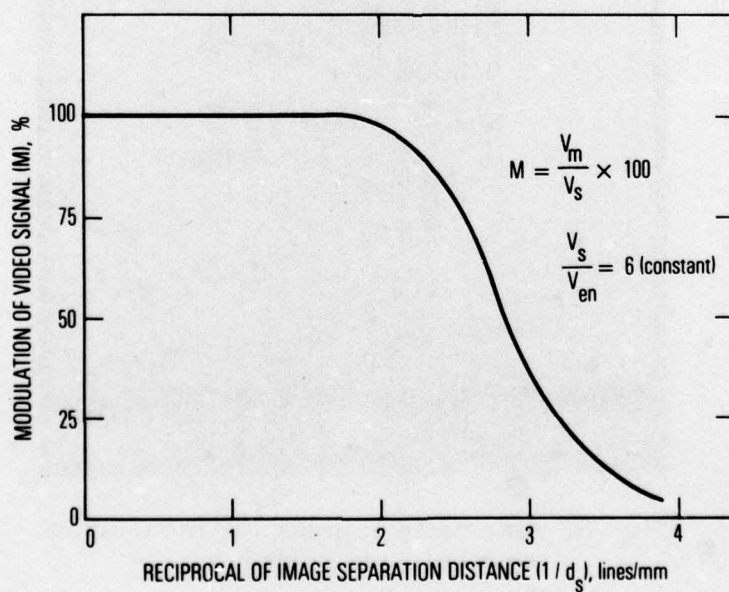-density filter magazine are placed in front of the aperture of a blackbody source that is focused on the image-sensing layer. Figure 11 is a photograph of the standard blackbody source, narrow band filter wheel, and neutral-density filter magazine used to verify this technique with mid-infrared image sensors.

The blackbody temperature is selected to provide a convenient V_s/V_{en} value through (1) a narrow band filter that transmits in the spectral region of anticipated maximum sensitivity for the image sensor and (2) neutral-density filters that attenuate radiant emittance from the blackbody source by almost three orders of magnitude. In this manner the blackbody temperature can be held constant. Only the neutral-density filtering is changed for each selected narrow band filter. For each narrow band filter selected the neutral-density filtering is decreased to the point where V_s/V_{en} is at the same value. Since the blackbody temperature, bandpass characteristics of each narrow band filter, optical parameters of the test configuration, and transfer characteristics of the image sensor are known, the NEH can be calculated for the wavelength region of each narrow band filter.

The measured spectral response data are presented as a semilog plot of the reciprocal of NEH in square centimeters per watt as a function of wavelength (λ) in microns. A typical spectral response curve is shown in Fig. 12. The NEH values were derived from the γ of the transfer characteristic curve and the measured H_s at each wavelength.

NARROW BAND
FILTER WHEEL

CALIBRATED
BLACKBODY
SOURCE

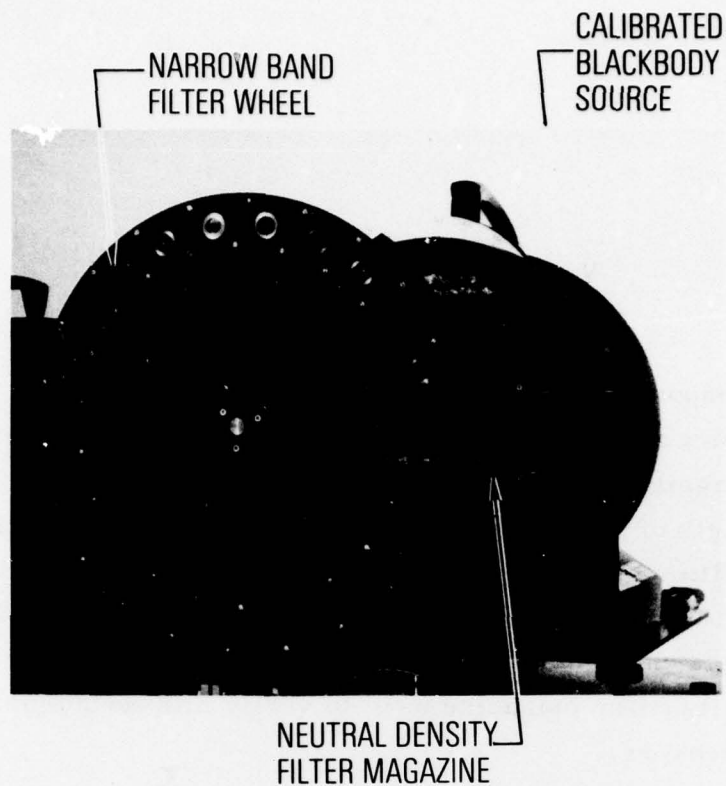NEUTRAL DENSITY
FILTER MAGAZINE

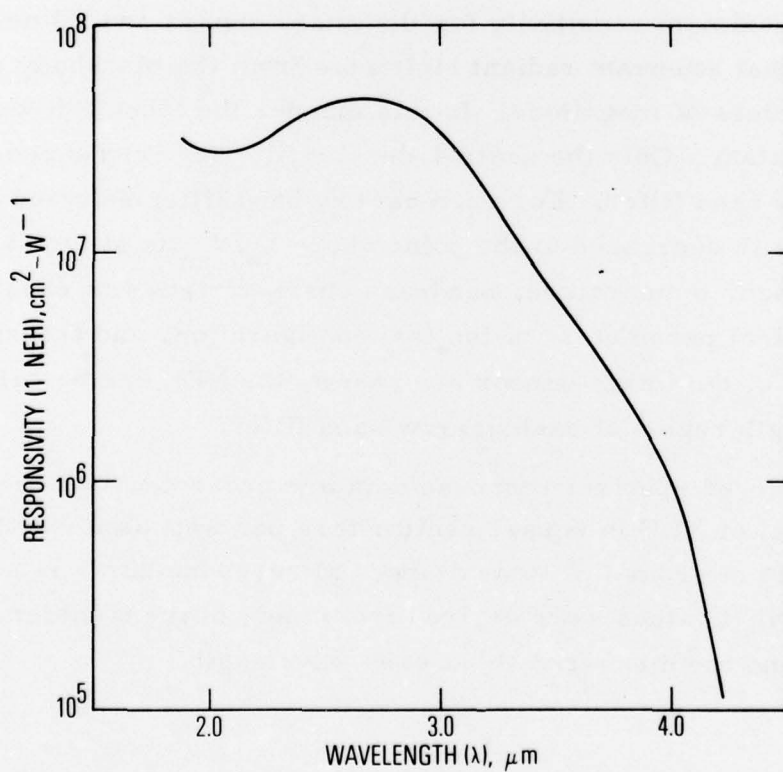Fig. 11. Laboratory setup to measure
spectral response

Fig. 12. Typical spectral response curve

VI. UNIFORMITY OF RESPONSE

Uniformity of response is the gradual variation in video output that is spatially related to the sensing-layer area. Variations are considered to be gradual if they comprise low-frequency voltage signals of less than 150 kHz when viewed on the line-selector oscilloscope. This parameter is determined by monitoring the V_s/V_{en} variations as a target of constant irradiance is positioned on various segments of the sensing layer. The typical target locations used to reliably measure response uniformity throughout a given sensing layer are shown in Fig. 13. This method is only useable for image sensors that have constant γ's. If γ is not constant throughout the sensing layer, a transfer curve must be taken at each target location.
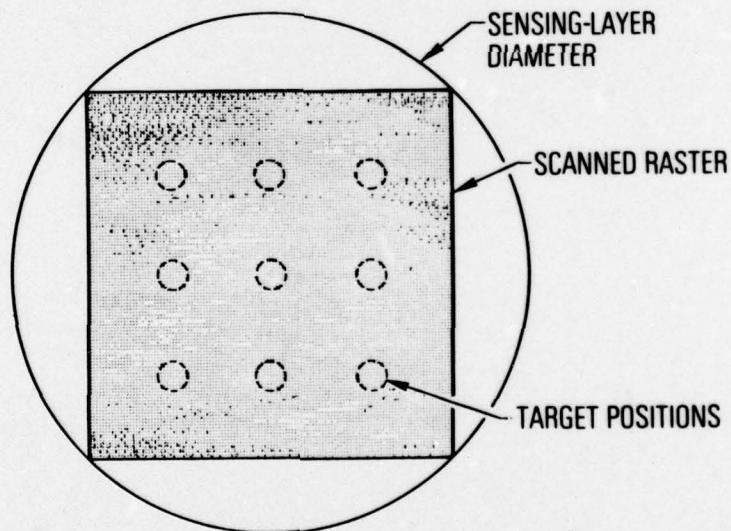
Fig. 13. Target position for response
uniformity measurements

VII. IMAGE RETENTION

Image retention is the time decay associated with the output video signal after instantaneous removal of a signal irradiance level. This parameter also can be described in terms of the number of frame times required to erase the V_s/V_{en} corresponding to an H_s value. Irradiance from a blackbody source is set up to produce a V_s/V_{en} linear portion of the image sensor's transfer curve. A polaroid camera is used to monitor the line-selector oscilloscope presentation of the target image. When the blackbody is shuttered, the decreasing V_s/V_{en} on each subsequent video scan can be photographed with the camera at a selected time exposure. A typical line-selector oscilloscope presentation, resulting from this method of determining image retention, is shown in Fig. 14. Since the video scan rate and camera shutter speed are known, the decreasing V_s/V_{en} can be plotted as a function of video signal off time (t). From this curve, retention time (t_{ir}) for an integrating image sensor is defined as the time required for V_s/V_{en} to decrease to 10% of the steady-state target signal.
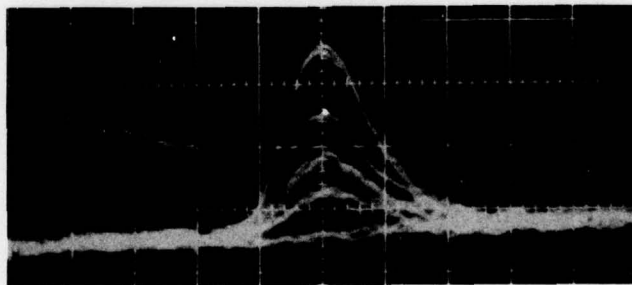

Fig. 14.   Line-selector-oscilloscope
presentation for image
retention measurement

VIII. CONCLUSIONS

The five figures of merit described provide a reliable evaluation of integrating image sensor performance. These criteria are applicable to a wide variety of imaging devices, including standard visible light vidicons, infrared camera tubes, Schottky-Barrier diode arrays, silicon diode vidicons, and some charge coupled arrays. The test method for each measurement can be accomplished with readily available laboratory equipment and can achieve a high level of quantitative accuracy.

LABORATORY OPERATIONS

The Laboratory Operations of The Aerospace Corporation is conducting experimental and theoretical investigations necessary for the evaluation and application of scientific advances to new military concepts and systems. Versatility and flexibility have been developed to a high degree by the laboratory personnel in dealing with the many problems encountered in the nation's rapidly developing space and missile systems. Expertise in the latest scientific developments is vital to the accomplishment of tasks related to these problems. The laboratories that contribute to this research are:

Aerophysics Laboratory: Launch and reentry aerodynamics, heat transfer, reentry physics, chemical kinetics, structural mechanics, flight dynamics, atmospheric pollution, and high-power gas lasers.

Chemistry and Physics Laboratory: Atmospheric reactions and atmospheric optics, chemical reactions in polluted atmospheres, chemical reactions of excited species in rocket plumes, chemical thermodynamics, plasma and laser-induced reactions, laser chemistry, propulsion chemistry, space vacuum and radiation effects on materials, lubrication and surface phenomena, photosensitive materials and sensors, high precision laser ranging, and the application of physics and chemistry to problems of law enforcement and biomedicine.

Electronics Research Laboratory: Electromagnetic theory, devices, and propagation phenomena, including plasma electromagnetics; quantum electronics, lasers, and electro-optics; communication sciences, applied electronics, semiconducting, superconducting, and crystal device physics, optical and acoustical imaging; atmospheric pollution; millimeter wave and far-infrared technology.

Materials Sciences Laboratory: Development of new materials; metal matrix composites and new forms of carbon; test and evaluation of graphite and ceramics in reentry; spacecraft materials and electronic components in nuclear weapons environment; application of fracture mechanics to stress corrosion and fatigue-induced fractures in structural metals.

Space Sciences Laboratory: Atmospheric and ionospheric physics, radiation from the atmosphere, density and composition of the atmosphere, aurorae and airglow; magnetospheric physics, cosmic rays, generation and propagation of plasma waves in the magnetosphere; solar physics, studies of solar magnetic fields; space astronomy, x-ray astronomy; the effects of nuclear explosions, magnetic storms, and solar activity on the earth's atmosphere, ionosphere, and magnetosphere; the effects of optical, electromagnetic, and particulate radiations in space on space systems.

THE AEROSPACE CORPORATION
El Segundo, California